1
Fluorescent Sterols for the Study of Cholesterol Trafficking in Living Cells

Avery L. McIntosh, Huan Huang, Barbara P. Atshaves, Stephan M. Storey, Adalberto M. Gallegos, Thomas A. Spencer, Robert Bittman, Yoshiko Ohno-Iwashita, Ann B. Kier, and Friedhelm Schroeder

1.1
Introduction

Cholesterol is one of the most important constituents in lipid microdomain (also known as lipid raft) formation in model [1] and plasma membranes [2]. Plasma membrane lipid rafts are not only enriched in cholesterol but also sphingolipids and phospholipids with saturated and monounsaturated fatty acyl chains [3]. The physical state of these microdomains is a distinct, liquid-ordered PM phase, intermediate between the fluid liquid-crystalline and rigid gel phases [3–15]. The existence, properties, and regulation of lipid rafts (reviewed in [3, 16–18]) provide a framework for the study of the location and function of membrane protein receptors, transporters, and downstream signaling molecules (Figure 1.1) that regulate uptake of cholesterol [19–42], fatty acids [43–45], glucose [19, 46–57], and other related processes [3, 21, 58–65].

Membrane lipid microdomains are a source of continuing complexity and frustration, as evidenced by the titles bestowed on recent reviews [16, 17, 65–75]. The range of sizes reported for lipid microdomains vary from the very small (1–10 nm) to the very large (>1 μm) [74, 76–79]. The small can be described as single annular shells of cholesterol surrounding lipids or proteins, that are refractory to biochemical isolation [74, 76, 80] while the larger domains, such as whole microvilli, filopodia, pseudopodia, basolateral, apical areas and bile canaliculi, are subject to biochemical isolation from tissues rich in polarized cells (liver, intestine, kidney) [79, 81–86].

The smallest microdomains can be localized within larger domains [87, 88], as elegantly shown for microvilli [89] but, in large part, intermediate-sized microdomains, 50–700 nm, have been the subject of most studies. Although morphologists observed the first intermediate-sized microdomains (50–100 nm), now termed caveolae, over 50 years ago [90, 91], their functional significance was uncertain until

Probes and Tags to Study Biomolecular Function. Lawrence W. Miller (Ed.)
Copyright © 2008 WILEY-VCH Verlag GmbH & Co. KGaA, Weinheim
ISBN: 978-3-527-31566-6

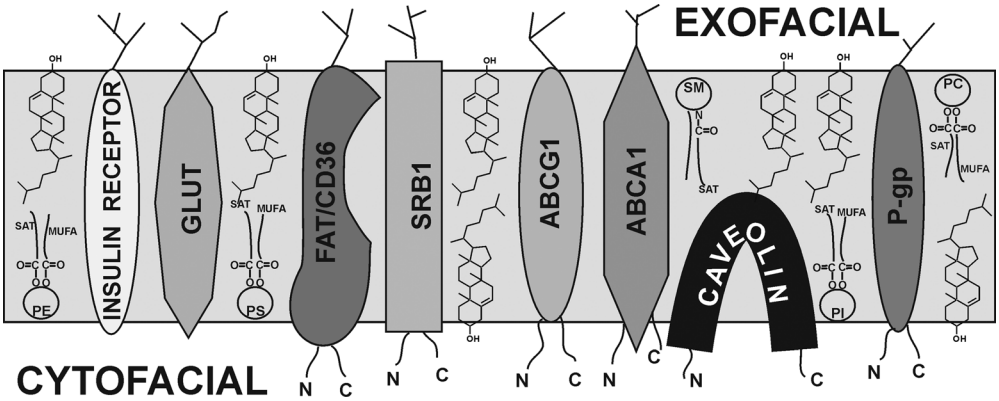

Figure 1.1 Cholesterol-rich microdomains within cellular plasma membrane. Membrane bilayer shows receptors and transport/translocase proteins distributed in lipid microdomains enriched in cholesterol.

the discovery of caveolin-1, the protein directing formation of this remarkably stable subclass of microdomain [17, 20, 36, 59, 61, 74, 75, 92, 93]. While caveolin provided the first convenient marker for biochemical isolation of caveolae, identical fractionation techniques also isolated similar size microdomains from cells lacking caveolin [20], indicative of "caveolae" as a subset of "lipid rafts" [94, 95]. Recently, emergence of many other types of "lipid rafts" has led to the appreciation that multiple intermediate-sized microdomains may coexist within the plasma membrane and likely in subcellular membranes as well. To clarify the growing complexity, a provisional definition of "lipid rafts" emerged at the 2006 Keystone Symposium: "Membrane rafts are small (10–200 nm), heterogeneous, highly dynamic, cholesterol- and sphingolipid-enriched domains that compartmentalize cellular processes. Small rafts can sometimes be stabilized to form larger platforms through protein–protein and protein–lipid interactions [18]." Lipid raft quantity (none to nearly the entire membrane [96]) and purity vary depending on the isolation techniques, with those obtained as detergent-resistant membranes (DRM) or high pH carbonate buffer-isolated membranes containing as much as 30–75% cross-contaminating non-raft and intracellular proteins [3, 4, 13, 16, 17, 68, 96–115]. DRMs can contain artifactual sterol structure (crystalline) and exhibit abnormal sterol efflux unresponsive to intracellular cholesterol transfer proteins [116].

Despite the obvious importance of cholesterol for lipid raft formation, very little is known regarding the actual properties of cholesterol itself within these microdomains. The lack of understanding of cholesterol's properties in microdomains underlines the importance of discovering and utilizing fluorescent sterol probes in living cells to study cholesterol trafficking, plasma membrane cholesterol organization (lateral, transbilayer, polar interface, order), dynamic interactions of cholesterol with lipids and proteins, and cholesterol transport in caveolae/lipid rafts [1, 10, 14, 17, 65, 117–119].

1.2
Methods for Imaging Fluorescent Sterols in Living Cells: Confocal and Multiphoton Laser Scanning Microscopy

1.2.1
Sources of Cholesterol and Fluorescent Sterols

Cholesterol is available from several commercial sources, e.g., AvantiPolar Lipids, (Alabaster, AL) (Figure 1.2A); 22-NBD-cholesterol or 22-(*N*-(7-nitrobenz-2-*oxa*-1, 3-diazol-4-yl)amino)-23,24-bisnor-5-cholen-3β-ol (Figure 1.2C) from Invitrogen (Carlsbad, CA), 25-NBD-cholesterol or 25-(*N*-[(7-nitrobenz-2-*oxa*-1,3-diazol-4-yl)-methyl]amino)-27-norcholesterol (Figure 1.2E) from AvantiPolar Lipids (Alabaster, AL). DChol or dansyl-cholesterol (Figure 1.2D) was synthesized as described [120]. BODIPY-Chol 2 with (4,4-difluoro-4-bora-3a,4a-diaza-*s*-indacene) located in the aliphatic tail of cholesterol (Figure 1.2F) was synthesized as described earlier [121]. DHE or dehydroergosterol (Figure 1.2B) is available from Sigma (St. Louis, MO) or was synthesized as described earlier [122–124]. FCBP or 22-(*p*-benzoylphenoxy)-23,24-bisnorcholan-5-en-3b-ol (Figure 1.2G) was synthesized as described earlier [125]. BCθ was derived by biotinylation of the protease-nicked θ-toxin [126, 127]. Purity of some fluorescent sterols was determined through the use of absorption spectroscopy, HPLC, and APCI-mass spectroscopy [128, 129]. Other sterols were accepted as per commercial sources or as cited in published papers.

1.2.2
Spectral Properties of Fluorescent Sterols

A Cary 100 (Varian, Palo Alto, CA) was used to acquire fluorophore absorbance spectra. Typical scans were acquired over the wavelength range, 200–600 nm, using quartz cuvettes. The fluorescence excitation and emission spectra of the fluorophores were obtained in quartz cuvettes with a Cary Eclipse spectrofluorometer (Varian, Palo Alto, CA) using a pulsed xenon lamp and analog detection mode. Emission and excitation monochromator slits were set at 5 nm spectral bandwidth.

1.2.3
Fluorescent Sterol Labeling Methodology

1.2.3.1 Method 1: Direct Labeling

Stock solutions were made by dissolving the fluorescent sterol in ethanol which was subsequently stored under N_2 at −80 °C. Intact L-cell fibroblasts were cultured as described previously in serum-containing medium on LabTek two-chambered coverglasses (VWR, Sugarland, TX) overnight [128]. After overnight growth, the medium was removed. For DHE and dansyl cholesterol the cells were incubated with the probe in serum-containing medium at 37 °C for times dependent upon the particular sterol and maintained at 5% CO_2 and subsequently imaged in PBS using laser scanning

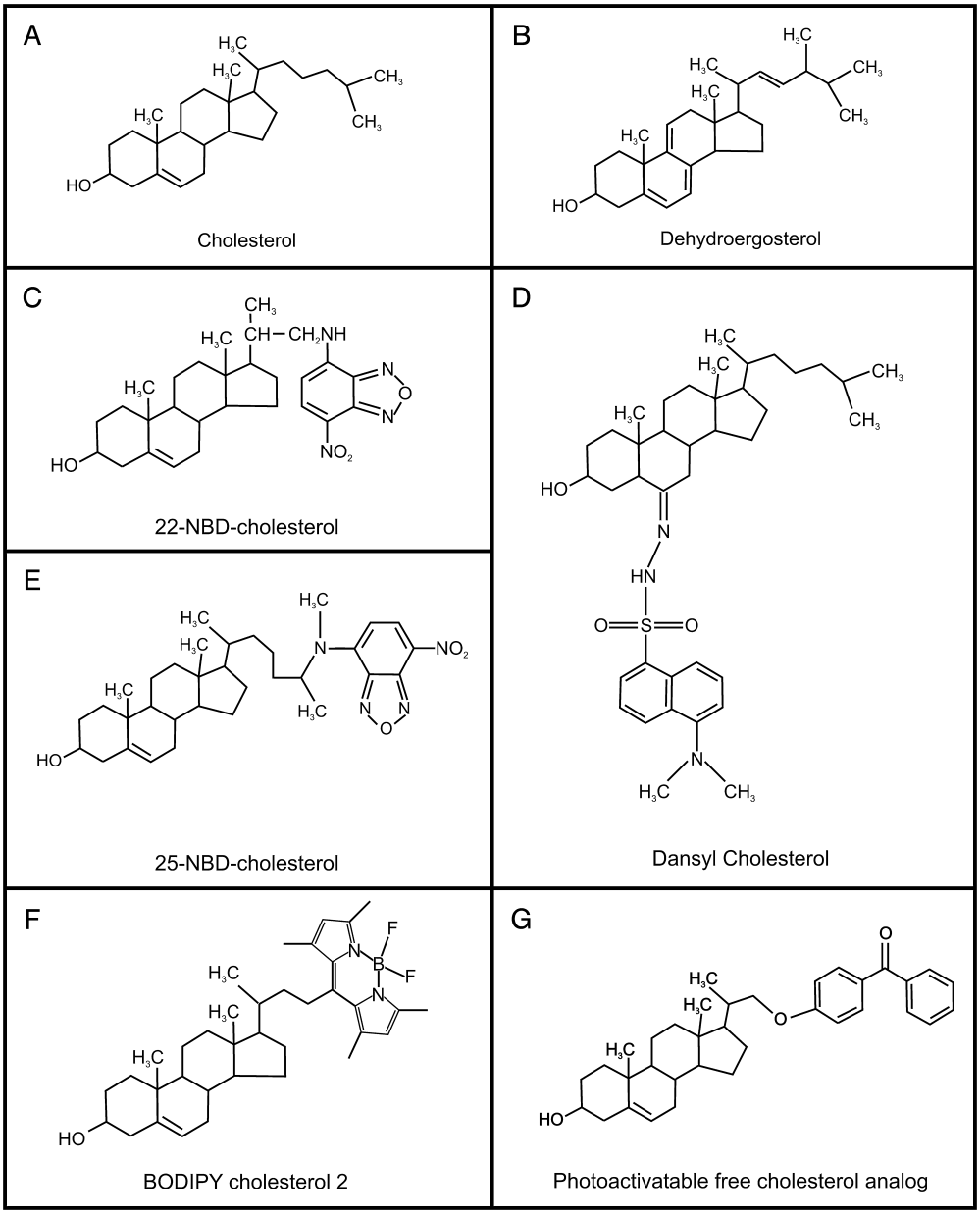

Figure 1.2 Structures of fluorescent sterol analogs. (A) cholesterol (B) dehydroergosterol (C) 22-NBD-cholesterol (D) Dansyl-cholesterol (6-dansyl-cholestanol) (E) 25-NBD-cholesterol (F) BODIPY-cholesterol-2 (G) FCBP photoactivatable sterol cross-linker.

microscopy as described below. In the case of the two moieties of NBD-cholesterol, the cells were washed with PBS and the fluorescent sterol was incubated in PBS while the resultant uptake was monitored by confocal laser scanning microscopy. For all sterols, the fluorescent sterol was added from an ethanolic stock solution so that the amount of ethanol was less than 0.2%.

1.2.3.2 **Method 2: Fluorescent Sterol Incorporation by Large Unilamellar Vesicles**

As described previously, large unilamellar vesicles (LUVs) were prepared by mixing 1-palmitoyl-2-oleoyl-*sn*-glycero-3-phosphocholine (POPC), 1,2-dioleoyl-*sn*-glycero-3-[phospho-L-serine] (DOPS) (Avanti Polar Lipids, Alabaster, AL), and the fluorescent probe from stock solutions in chloroform in the proportions 65 mol% POPC, 35 mol % sterol, and 10 mol% DOPS unless otherwise stated [128]. The lipid mixture was first dried under N_2 and then *in vacuo* overnight. Then 10 mM PIPES (1,4-piperazinediethanesulfonic acid) buffer at pH 7.2 was added, followed by sonication for 10 min. The multi-lamellar vesicles were then extruded using a Mini-Extruder (Avanti Polar Lipids, Alabaster, AL), producing large unilamellar vesicles with median radii 53 ± 10 nm. L-cells were cultured on chambered coverglasses in serum-containing media and then washed three times with PBS. Subsequently, an aliquot of LUVs was added to the L-cells in PBS so that the cells were incubated overnight with 20 μg of sterol, except in the case of DHE where the cells were incubated with LUVs in serum-containing media. Prior to imaging the cells were washed three times with PBS and then imaged in PBS.

1.2.3.3 **Method 3: Fluorescent Sterol-methyl-β-cyclodextrin (FS-MβCD) Complexes**

The fluorescent sterol-MβCD complex was prepared in a 1 : 3 ratio of fluorescent sterol : MβCD by mixing the fluorescent sterol as a powder in an aqueous solution of MβCD. The vessel was filled with N_2 and continuously vortexed under light protection for 24 h at room temperature. The solution was filtered through a 0.2 μm filter to remove insoluble material and large aggregates before use. The fluorescent sterol-MβCD complex was then added to the cells and incubated for 45 min at room temperature in PBS. The cells were subsequently washed three times with PBS and imaged by laser scanning microscopy in PBS.

1.2.3.4 **Method 4: Fluorescent Labeling of High Density Lipoproteins (HDL)**

A previously published protocol [130] was modified for the fluorescent labeling of high density lipoproteins. The lipids, 2.3 μmol egg phosphatidylcholine, 0.6 μmol sphingomyelin, 2.24 μmol fluorescent sterol, 0.6 μmol cholesterol, and 0.34 μmol triolein, were mixed in chloroform, dried under nitrogen, and then *in vacuo* overnight. 5 ml of a buffer composed of 10 mM Tris-HCl, pH 8.0, 150 mM NaCl, and 0.25 mM EDTA was added and the mixture was vortexed and sonicated at 52 °C for 40 min. 5 ml of HDL in 1 ml of a new buffer (addition of 2.5 M urea in the previous buffer), was added drop-wise over 5 min at 42 °C and sonicated for 10 min at 52 °C. The supernatant was collected after centrifugation and centrifuged again using a sucrose gradient. Neighboring fractions containing the highest amounts of lipoproteins and the fluorescent sterol (determined by

Western blotting and fluorescence emission spectra) were consolidated for cell labeling.

Primary murine hepatocytes were cultured on collagen-coated Nalge Nunc Lab-Tek two-chamber coverglasses overnight in complete media at 37 °C with 5% CO_2. The hepatocytes were washed twice with warm PBS and stabilized for 15 min in 800 µl of PBS at 37 °C with 5% CO_2, followed by incubation of the fluorescently labeled HDL in 200 µl of PBS.

1.2.3.5 **Method 5: BCθ**

L-cell fibroblasts were cultured as described previously in serum-containing media on LabTek two-chambered coverglasses (VWR, Sugarland, TX) overnight [128]. After overnight growth, the medium was removed, washed with PBS, and further incubated with PBS containing BCθ (10 µg ml^{-1}) and 1 mg ml^{-1} fatty-acid-free bovine serum albumin (BSA) at room temperature for 20 min. The cells were washed three times with PBS and then incubated with FITC-Avidin 40 µg ml^{-1} in PBS with BSA at room temperature for another 20 min. The cells were again washed three times with PBS and imaged in PBS.

1.2.4 Confocal Laser Scanning Microscopy (CLSM) and Multiphoton Laser Scanning Microscopy (MPLSM) of Sterol Probes

Synthetic (dansyl-, NBD-, BODIPY-, FCBP), naturally-occurring (DHE), or BCθ probes of cholesterol were incorporated as described above in order to monitor the cholesterol microenvironments within membranes of living L-cells. These fluorescent sterols or sterol probes were imaged in real time by confocal laser scanning microscopy (CLSM) or multiphoton laser scanning microscopy (MPLSM) using a MRC-1024MP Confocal/Multiphoton imaging system (Zeiss, Thornwood, NY), coupled to a Zeiss Axiovert 135 inverted microscope (Zeiss, Thornwood, New York) using either of these Zeiss oil immersion objectives: 40X Apochromat 1.4 NA, a 63× Plan-Apochromat 1.4 NA, or a 100× Fluar 1.3 NA. For CLSM of NBD- and BODIPY-cholesterols the intrinsic excitation system consisted of an Ar^+/Kr^+ ion laser providing a laser line of 488, 568, and 647 nm lines of 3–4 mW at the fiber output. For excitation of the dansyl fluorophore, the system was modified with the addition of a 30 mW temperature stabilized 408 nm diode laser (Power Technology, Little Rock, AR) with beam circularization using anamorphic prisms for excitation. An internal HQ530/40 dichroic filter (Chroma Technology, Rockingham, VT) was used in conjunction with fluorophores emitting in the green wavelength region. For MPLSM of DHE, sub-picosecond multiphoton excitation was provided by a mode-locked Coherent Mira 900F (Coherent, Palo Alto, CA) tuned to 900 nm. The 900 nm infrared pulsed laser light was focused in confocal planes within the cell with the *z*-axis control. The fluorescence emission from the multiphoton excitation volume was collected by the objective and reflected out of the microscope along the excitation path. Inside the external detector system obtained from Dr. Warren Zipfel (Cornell University, Ithaca, NY), the fluorescence emission was separated from the excitation

path with a 670UVDCLP dichroic. Emission was split among three dichroics/filter combinations with corresponding photomultiplier tubes. The three dichroics and emission filters permitted selection of different wavelength/bandwidth regions in three channels. The following three emission filters (Chroma Technology, Rockingham, VT) were used to image DHE in living cells: a filter centered at 375 nm with a 50 nm bandwidth for detection of the higher intensity of the monomeric form; a filter centered at 455 nm with a 30 nm bandwidth for detection of the higher intensity of the microcrystalline form; a filter centered at 400 nm with a 100 nm bandwidth for collecting a significant portion of the DHE spectral emission. Ratioing the intensities from the 455 nm channel to that of the 375 nm channel provides information about the proportion of monomeric to crystalline sterol. In the case where there is no accumulation of the crystalline form, the larger bandwidth enhances the sensitivity by integrating the fluorescence intensity over a larger emissive wavelength region. For the FCBP, a BGG 22 filter was used in combination with a 500 DCLP to cover the range 410–490 nm. Typically four images were averaged using a kalman filter in order to reduce the noise.

1.3
Cholesterol Structure and Distribution in Membranes

The structure of cholesterol consists of a cyclopentanoperhydrophenanthrene type center with a 3-hydroxy group, two methyl groups, a C-5,6 double bond, and an aliphatic side chain with methyl groups (Figure 1.2A) with formula weight $C_{27}H_{46}O$. Cholesterol distributes laterally, not only as cholesterol-rich phases, but also as small clusters (10–25 nm) in model and biological membranes [119, 131, 132], although these cholesterol clusters do not represent cholesterol crystals [128, 133]. The function of these clusters relates to the ability of cholesterol to form a hexagonal phase [134], possibly accounting for the very rapid spontaneous transbilayer migration rate of cholesterol ($t_{1/2}$ = seconds to minutes) in most model and plasma membranes [135–141]. Whether lipid rafts consist of enrichment of these small cholesterol clusters remains unknown.

Consistent with the lower exposure of the cholesterol headgroup (OH) to the aqueous interface in tightly-packed, more highly-ordered membrane regions [65], cholesterol-rich membranes such as lipid rafts have increased transbilayer thickness [2, 142]. Structurally, the degree of cholesterol headgroup aqueous exposure at the membrane/aqueous interface is expected to significantly affect cholesterol desorption/uptake between microdomains and extracellular serum lipoproteins or intracellular cholesterol binding proteins. In bulk plasma membrane analysis, cholesterol has been observed to reside in two microenvironments [84, 143–146]: a more aqueous exposure wherein 10–40% has a long fluorescence lifetime with exchangeable sterol and less exposure wherein 60–90% has a short lifetime with very slowly exchangeable sterol.

Though the transbilayer distribution of cholesterol in lipid rafts remains enigmatic, enrichment in the cytofacial leaflet has been shown indirectly, based upon known

localization of other lipids (sphingomyelin (SM) and GM1 in the exofacial leaflet) and cross-linking of GM1 with SM, but not in DRMs [147]. It has been shown that 80–90% of cell cholesterol is in plasma membranes [84], generally distributed in the cytofacial leaflets, as observed both in purified plasma membranes and in intact cells [85, 135, 139, 140, 148–150]. At equilibrium, not only the flip-flop rate, but also phospholipid species, acyl chain unsaturation, and cholesterol–protein interactions contribute significantly to determining the transbilayer cholesterol distribution. For example, some model membrane studies suggest that cholesterol binds phospholipids in the order SM > PS > PC > PE [151], while others show that this order is highly dependent on the specific acyl chain composition (saturated vs. unsaturated) [144, 152]. Thus, while SM is known to be enriched in the plasma membrane outer leaflet [153], whether cholesterol preferentially interacts with SM therein is highly dependent on the acyl chain composition, not only of SM but also of the other phospholipids present in the cytofacial as well as the exofacial leaflets. Enrichment of plasma membrane phospholipids with polyunsaturated fatty acids (PUFAs) esterified to classes other than SM significantly alters transbilayer cholesterol distribution [154, 155]. Cholesterol also preferentially binds with specific membrane proteins. These findings are consistent with the crucial element in cholesterol distribution being the formation of highly packed lipid structures, rather than specific complex formation between SM and cholesterol [144, 156].

Cholesterol efflux from model membranes [84, 143, 145, 146, 157, 158] and plasma membranes [84, 85] has been shown to have two kinetically and structurally resolvable components ($^1t_{1/2}$ = minutes to hours, $^2t_{1/2}$ = days). Since model and plasma membrane cholesterol transbilayer migration rates are rapid (seconds to minutes) [135, 139, 140, 159–161], these cholesterol domains represented lateral, rather than transbilayer, lipid rafts [84, 85, 162, 163]. Slower cholesterol efflux from less fluid model membranes would suggest that rapidly transferable cholesterol must be associated with non-rafts in model membranes [40, 84]. Contrary to expectations, however, cholesterol efflux from plasma membrane lipid rafts was much faster than from non-rafts, suggesting that cholesterol in lipid rafts from biological membranes may not be organized like model membrane microdomains.

Clearly, more studies need to be performed in order to understand fully the interactions of cholesterol with its neighboring lipids and proteins in living membranes and several fluorescent sterol probes have been developed to study different aspects of cholesterol and can be applied to imaging its nature in living cells (Figure 1.2B–G).

1.4 NBD-Cholesterol

The NBD group typically has a broad excitation range that can easily be excited at the 488 nm Ar^+ ion laser line with relatively high emission intensity over the region 500–600 nm (Table 1.1) depending upon the polarity of the environment of the probe. In aqueous buffers, the NBD group of the cholesterol analog exhibits a fluorescence

Table 1.1 Fluorescent cholesterol analogs used in microscopic imaging of living cells.

	Excitation Maximum (nm)		Emission Maximum (nm)		
Sterol	**EtOH**	**Aqueous**	**EtOH**	**Aqueous**	**Comments**
DHE	311, 324, 340	314, 329, 340	354, 371, 390 (VL)	356, 375, 403, 426 (L)	naturally-occurring, fluidity sensitive, prefers lipid rafts microcrystalline appears in aqueous and lysosomes
NBD-chol	334, 467	425–507	531 (M-H)	550–650 (L)	polarity and fluidity sensitive
BODIPY Chol 2	496	572	504 (H)	573 (M-H)	prefers lipid rafts
Dansyl-chol	336	342	517 (M-H)	506 (L-M)	polarity sensitive, prefers lipid rafts
FCBP	(230, 250, 292)[a] (246, 311)[b]		333, 445 (VL)	ND	photoactivatable, Prefers lipid rafts, binds caveolin

ND = not detectable. Emission yields: VL = very low; L = low; M = medium; H = high.
[a]Excitation maxima for emission collected at 333 nm.
[b]Excitation maxima shifts to 246 and 311 nm when collecting emission at 445 nm.

emission maximum at ∼545 nm but shifts to ∼533 nm in ethanol (Table 1.1). Two moieties of cholesterol labeled in the alkyl side chain are easily obtainable: 22-(*N*-(7-nitrobenz-2-*oxa*-1,3-diazol-4-yl)amino)-23,24-bisnor-5-cholen-3β-ol (22-NBD-cholesterol, Figure 1.2C) and 25-(*N*-[(7-nitrobenz-2-*oxa*-1,3-diazol-4-yl)-methyl]amino)-27-norcholesterol (25-NBD-cholesterol, Figure 1.2E).

1.4.1 22-NBD-Cholesterol

22-NBD-cholesterol was easily incorporated into living cells by direct addition from a stock solution (Figure 1.3A) and by using methyl-β-cyclodextrin complexes (Figure 1.3B); as determined by confocal laser scanning microscopy (CLSM). The images reveal very little propensity for this moiety to be visualized within the L-cell plasma membrane – the cellular membrane with the highest cholesterol content (reviewed in [3, 84–86, 162]. In model membranes composed of dimyristoylphosphatidylcholine (DMPC) and cholesterol, 22-NBD cholesterol was shown to prefer the cholesterol-poor l_d phase as opposed to the cholesterol-rich l_o phase. Using dithionite-mediate quenching of the 22-NBD-cholesterol fluorescence at 30 °C in large unilamellar vesicles of 1-palmitoyl-2-oleoyl-*sn*-glycero-3-phosphocholine (POPC-LUV), the NBD group was partially exposed at the water, suggesting either bending of the flexible alkyl side chain (to which NBD is attached) or potentially an

inverted configuration when compared to cholesterol [164]. Although these studies suggested that 22-NBD-cholesterol might insert poorly/weakly into lipid bilayers, other studies showed that 22-NBD-cholesterol was bound with high affinity (nM) by intracellular lipid binding proteins (SCP-2, ADRP) and was bound to these proteins with orientation similar to cholesterol [162, 165–169]. These data indicated that 22-NBD-cholesterol might be a more suitable probe for cholesterol uptake/trafficking

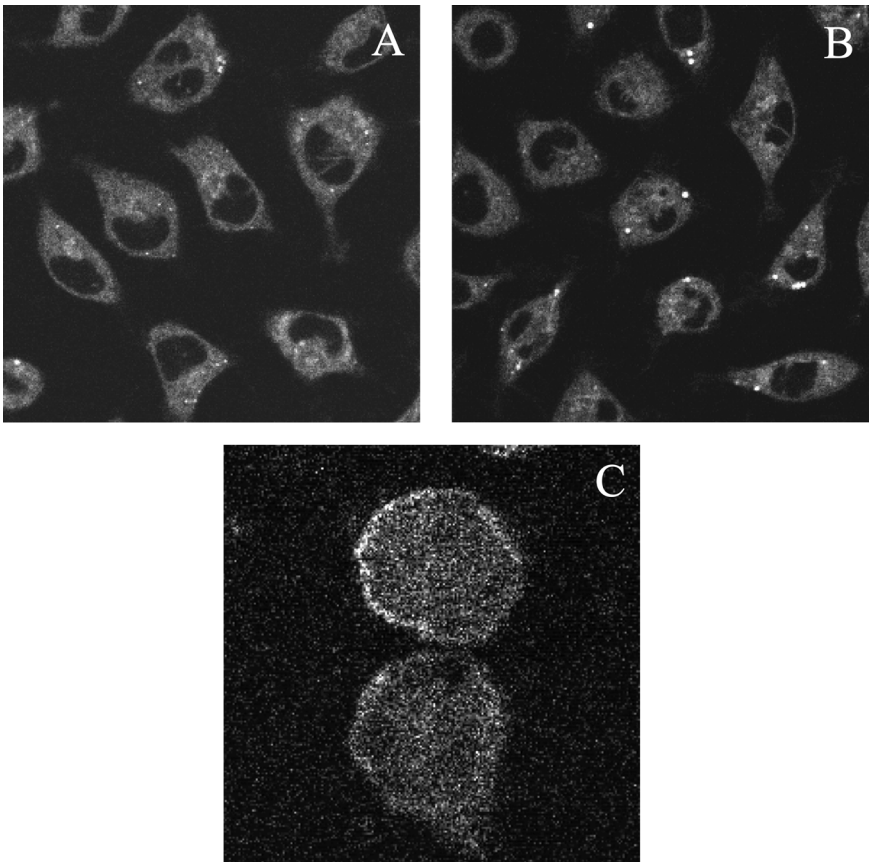

Figure 1.3 CLSM of the 22-NBD-Cholesterol in living cells by three methods. (A) Direct addition: 22-NBD-Chol from a stock solution in EtOH was added to PBS (% EtOH was kept under 0.2% v/v). L-cells, cultured on chambered coverglass, were incubated with the 22-NBD-Chol in PBS so that the incubation concentration was 0.2 μM. Incubation occurred at room temperature for 30 min. (B) 22-NBD-Chol-MβCD complexes: L-cells were incubated with NBD-Chol-MβCD complexes so that the total NBD-cholesterol concentration was 0.6 μM in PBS at room temperature for 40 min. Images were collected as in (A) but with approximately threefold less power. (C) 22-NBD-Chol-HDL complexes: Primary mouse hepatocytes from C57BL/6 mice were incubated in PBS at 37 °C for 30 min with high density lipoproteins loaded with 22-NBD-Cholesterol (0.4 μM) as described in Method 4. All images acquired by CLSM with 488 nm laser excitation and emission detection through a HQ530/40 filter. Zeiss 63× oil immersion objective used in (A) and (B) and the Zeiss 40× oil immersion objective used in (C).

than plasma membrane insertion, at least in cultured L-cell fibroblasts. Consistent with this possibility, 22-NBD-cholesterol cellular uptake rates were >100-fold faster than [^{3}H] cholesterol due to selective uptake via the high density lipoprotein (HDL) receptor mediated pathway [170]. The 22-NBD-cholesterol rapidly enters the living cell and targets lipid droplets through non-vesicular mechanisms [170]. Similarly, efflux of 22-NBD-cholesterol was HDL-mediated with rates much faster than with [^{3}H] cholesterol. Interestingly, although sterol carrier protein-2 (SCP-2) enhanced uptake, it was shown to inhibit the effects of extracellular HDL [169] during efflux, revealing the protein's potential involvement in cellular cholesterol homeostasis [169]. Kinetic analysis of 22-NBD-cholesterol efflux from the cytoplasm of cultured L-cells reveals two dynamic pools: (i) a small (18%), very rapid ($t_{1/2} = 1.9$ min) pool reflecting protein-mediated cholesterol trafficking, and (ii) a large (82%), slower ($t_{1/2} = 14.7$ min) pool reflecting vesicular cholesterol trafficking [169]. Overexpression of sterol carrier protein-2 (SCP-2), which binds 22-NBD-cholesterol with high affinity [162, 165, 166], dramatically accelerated (reduced $t_{1/2}$ to 1.4 min) the rapid, protein-mediated transfer without affecting its pool size. In contrast, SCP-2 overexpression decreased (increased $t_{1/2}$ to 31.4 min) the slower, vesicular transfer – again without affecting its pool size [169]. The latter observation correlated with the ability of SCP-2 to bind and sequester phosphatidylinositides [171, 172] and fatty acyl CoAs [173, 174], both of which are known to regulate vesicular trafficking (reviewed in [175–177]). Incubating primary cultured mouse hepatocytes with high density lipoproteins labeled with 22-NBD-cholesterol, the fluorescent cholesterol analog localizes early into the plasma membrane (Figure 1.3C).

22-NBD-cholesterol has been incorporated into macrophages and lymphocytes obtained from rats. Differences in uptake were examined based upon thioglycollate-injected rats and control rats as well as those stimulated *in vitro* by lipopolysaccharide and phorbol-myristate acetate and compared with concanavalinA treatments which did not appear to modulate cholesterol incorporation by lymphocytes. Thioglycollate-treated macrophages revealed higher initial uptake of NBD-cholesterol [178].

1.4.2
25-NBD-Cholesterol

25-NBD-cholesterol was also easily incorporated into living cells by direct addition from a stock solution (Figure 1.4A) with similar results and no labeling of the plasma membrane even after 30 min (Figure 1.4B–D). However, by using methyl-β-cyclodextrin complexes (Figure 1.5), the plasma membrane was labeled significantly in the first 2 min (Figure 1.5A) but with subsequent diminishment in intensity (Figure 1.5B and C), especially after 10 min as the probe was internalized (Figure 1.5D). The orientation of 25-NBD-cholesterol in membranes is controversial. In model membrane POPC-LUVs, a quenching effect similar to 22-NBD-cholesterol was observed using dithionite quenching, again suggesting either bending of the cholesterol alkyl chain (with attached NBD) toward the bilayer surface or possibly an inverted orientation as compared to cholesterol [164]. However, another study revealed that a second population of sterol in dipalmitoylphosphatidylcholine (DPPC) membranes

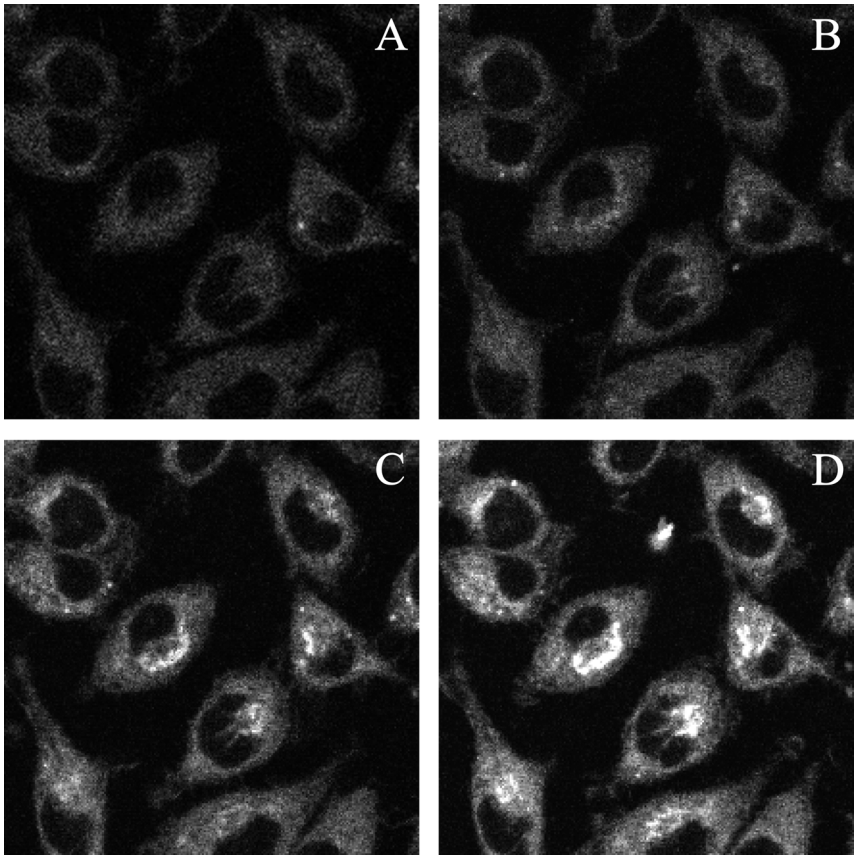

Figure 1.4 Uptake of 25-NBD-cholesterol in living cells by direct addition. 25-NBD-cholesterol from a stock solution in EtOH was added to PBS (% EtOH was kept under 0.2%v/v). L-cells were incubated with 25-NBD-Chol in PBS (incubation concentration of 0.6 μM) at room temperature for (A) 5, (B) 10, (C) 20, (D) 30 min. Images were acquired using CLSM with 488 nm laser excitation and emission detection using a HQ530/40 nm emission filter.

interacted in a tail-to-tail dimer configuration across the membrane bilayer [179]. The intracellular distribution of 25-NBD-cholesterol was reported to be different from that of the 22-NBD-cholesterol with most of the 25-NBD-cholesterol targeting mitochondria [180] in a Chinese hamster ovary (CHO) cell line, as determined by video fluorescence imaging.

In a depth-dependent solvent relaxation study involving the effects of polarity on low amounts of 25-NBD cholesterol within reverse micelles of sodium bis(2-ethyl-hexyl) sulfosuccinate (AOT) formed in isooctane, although the maximum remained at 513 nm with excitation at 475 nm with increasing amounts of water/AOT ratio, the increasing polarity created an increase in the red edge excitation shift as well as decreases in the intensity maxima and in both components of the fluorophore

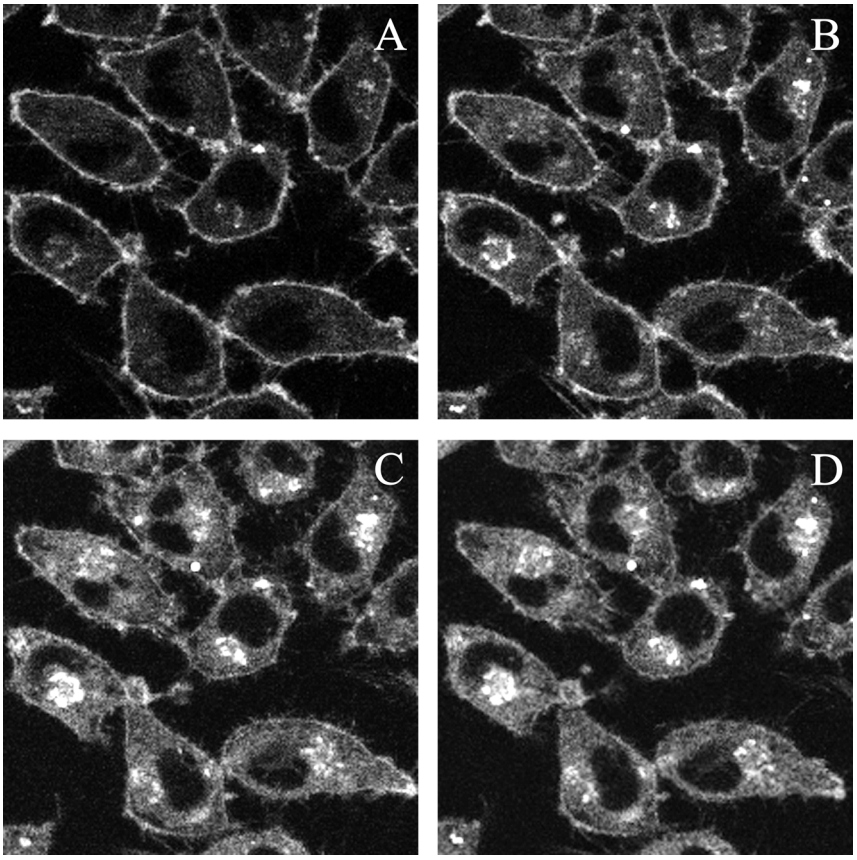

Figure 1.5 Uptake of 25-NBD-cholesterol in living cells using MβCD complexes. L-cells were incubated with 25-NBD-Chol-MβCD (incubation concentration of 25-NBD-cholesterol of 0.6 μM) in PBS at room temperature for (A) 2, (B) 5, (C) 10, (D) 15 min. Images were acquired using CLSM with 488 nm laser excitation and emission detection using a HQ530/40 nm emission filter. CLSM conditions were similar to those in Figure 1.4.

lifetime. With the increase in the water/AOT ratio of 0–25, the red edge excitation shift changed from 6 to 11 nm, reflecting restricted motion as a possible indicator of the fluorophore's location well below the surface [181].

1.5 Dansyl-Cholesterol

Dansyl-cholesterol (DChol) was synthesized recently and used in the study of plasma membrane-derived cholesterol transport involving the Niemann-Pick C1 (NPC1) protein in cultured cells [120]. The structure (Figure 1.2D) of the new probe was that of a cholesterol labeled with the fluorescent dansyl group (5-dimethylamino-1-

naphthalenesulfonyl) attached at carbon position 6 to form the 6-dansyl-cholestanol [120]. In ethanol, the dansyl group has broad excitation with a peak maximum at 336 nm with broad greenish emission peaking at 522 nm (Table 1.1). The emission yield was quite high but photobleaching was significant under high excitation powers. In aqueous buffer with pH 7.4, the DChol emission peak was shifted to 506 nm. Under low pH ∼ 1–2, the intensity decreased with a wavelength shift to 490 nm. In lipid bilayers, the dansyl polar group of dansyl lipid probes was shown to reside 19–21 Å from the bilayer center and was sensitive to its environment, creating shifts in the wavelength [182]. CLSM (described above) was performed using a 408 nm laser for excitation and a HQ530/40 nm dichroic emission filter. DChol can be incorporated into living cells by direct addition with incubation periods of 1–2 h (Figure 1.6A), by complexation with methyl-β-cyclodextrin (DChol-MβCD) with short incubation times (Figure 1.6B), and by feeding the cells with LUVs composed of a mixture of POPC:DChol:PS (Figure 1.6C). In all three cases, plasma membrane labeling was evident – especially when the DChol was delivered to the cells as DChol-MβCD complexes or by LUVs.

The DChol probe with the dansyl group located away from the aliphatic side chain and the 3β-OH group (Figure 1.2D) produced different results, unlike the NBD labeled sterols [120]. DChol, in the form of DChol-MBCD complexes, along with [^{3}H] cholesterol was used to label CHO cells and the efflux kinetics, raft association, and esterification rate were measured [120]. The results of the comparisons for uptake and intracellular esterification showed DChol to differ only slightly from [^{3}H] cholesterol in CHO cells [120]. The dansyl cholesterol was reported to traffick to the endoplasmic reticulum with some cells showing accumulation in the Golgi but most going to lipid droplets [120]. The rate of accumulation in lipid droplets seemed to suggest that it was unesterified DChol that appeared at early times [120].

In another study [183] illustrating the different reverse transport pathways of LDL-cholesterol and acetylated LDL-cholesterol, an Olympus IX 70 inverted fluorescence microscope and Imago charge-coupled device was used to observe DChol in fetal liver-derived and bone marrow-derived mouse macrophages. LDL and AcLDL was labeled with DChol and incubated with wild-type and ABCA1-knockout mice-derived macrophages and the results compared to [^{3}H] cholesterol [183]. The LDL-DChol was observed to be transported diffusely through cellular membrane regions whereas the AcLDL-DChol was observed to go to late endosomes [183].

1.6 BODIPY-Cholesterol

Several BODIPY-labeled free cholesterol analogs were synthesized with the hydrophobic BODIPY fluorophore (4,4-difluoro-4-bora-3a,4a-diaza-*s*-indacene) located in the aliphatic tail [121]. Since the spectral characteristics of the BODIPY include a high coefficient of absorption in the near green with a high quantum yield in the green (Table 1.1) as well as long term photostability, this sterol analog became very

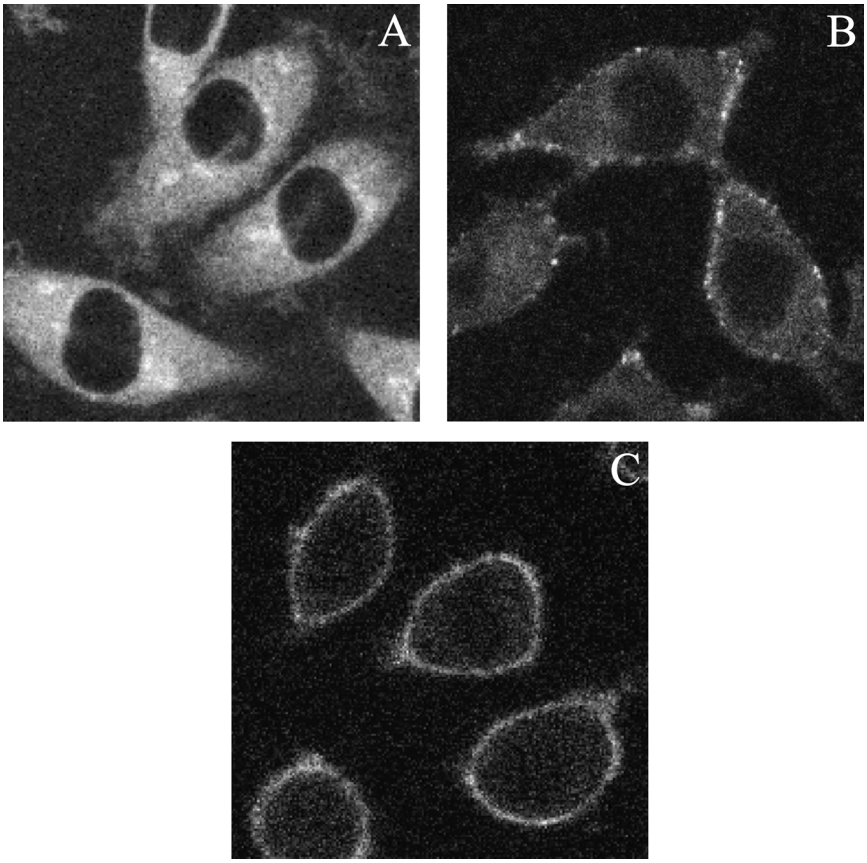

Figure 1.6 The distribution of dansyl-cholesterol within living cells after incubation by three different methods. All images were acquired by CLSM using 408 nm diode laser excitation and a HQ530/40 nm emission filter. (A) Direct addition: Dansyl-cholesterol was added from a stock solution in EtOH to PBS such that the percent EtOH was kept under 0.2%v/v. L-cells were incubated with the Dansyl-cholesterol in PBS with a concentration of 20 μg ml^{-1} at room temperature for 2 h followed by image acquisition. (B) LUV: LUVs containing dansyl-cholesterol (POPC:DChol: DOPS = 55 : 35 : 10 mol%) were made as described in the Methods. L-cells in PBS were incubated with the dansyl cholesterol containing LUVs at 20 μg ml^{-1} at room temperature for 1 h; followed by image acquisition. (C) Dansyl-Chol-MβCD complexes: L-cells were incubated at room temperature with 0.6 μM dansyl-chol-MβCD in PBS for 30 min.

appealing, especially for use in CLSM, as seen in Figure 1.7. Two fluorescent cholesterol analogs, BODIPY-Chol 1, 22-[4-(4,4-difluoro-1,3,5,7-tetramethyl-4-bora-3a,4a,diaza-*s*-indacen-8-yl)butyroxy]-23,24-bisnorchol-5-en-3β-ol, (not shown) and BODIPY-Chol 2 23-(4,4-difluoro-1,3,5,7-tetramethyl-4-bora-3a,4a,diaza-*s*-indacen-8-yl)-24-norchol-5-en-3β-ol, (Figure 1.2F) were prepared with the BODIPY linked to the side chain with and without oxygen atoms, respectively, while a third was a BODIPY-coprostanol analog 23-(4,4-difluoro-1,3,5,7-tetramethyl-4-bora-3a,4a,diaza-

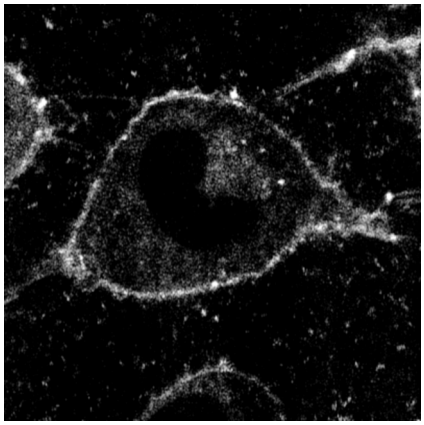

Figure 1.7 Localization of the raft preferring BODIPY-Chol-2 in living cells. LUVs containing BODIPY-Chol-2 (POPC : Chol : BODIPY-Chol-2 : DOPS = 63 : 26 : 7 : 4 mol%) were made as described in the Methods. L-cells in PBS were incubated with the BODIPY-Chol-2 containing LUVs at total sterol concentration 20 μg ml^{-1} at room temperature for 1 h; followed by CLSM image acquisition. Laser excitation was 488 nm with confocal emission detection using the HQ530/40 nm filter.

s-indacen-8-yl)-24-nor-5β-cholestan-3β-ol, (not shown) linked without oxygen atoms [121]. BODIPY-Chol 2 was observed to have ideal mixing in mixed monolayers of the compound with POPC [121]. Further characterization in multilamellar vesicles of the fluorescent sterol and saturated glycerophopholipids or sphingomyelin revealed that BODIPY-Chol 2 compared reasonably well with cholesterol in forming detergent-resistant sterol-rich domains while BODIPY-Chol 1 and 3 did not – suggesting that the BODIPY-Chol 2 might be a preferential probe of cholesterol-rich lipid rafts [121]. The cyclodextrin-mediated desorption rates of cholesterol and BODIPY-Chol 2 from monolayers mixed with POPC and the fluorescent analog were also similar [121].

Further studies using correlated fluorescence-atomic force microscopy revealed that BODIPY-Chol 1 and BODIPY-Chol 3 did not represent cholesterol in supported bilayers [184]. BODIPY-Chol 2 showed similarity with cholesterol but a dependence upon the type of sphingomyelin used: non-preferential distribution between l_o and l_d domains occurred when using *N*-stearoyl-D-*erythro*-sphingosylphophorylcholine (18 : 0) but there was preferential distribution into l_o domains using brain sphingomyelin and into l_d domains using the shorter 16 : 0 [184].

Two new BODIPY-labeled analogs of free cholesterol have been synthesized with an acetylenic linkage in the aliphatic portion of the cholesterol through either carbon position 8 or carbon position 5 of the BODIPY fluorophore [185]. In ethanol, the C8 bonded moiety showed an absorbance maximum of 499 nm and an emission maximum of 508 nm while linkage at the BODIPY C5 produced a significant red shift of 70 nm in the absorbance peak and a 75 nm red shift in the emission peak [185]. These compounds also exhibited high extinction coefficients, small Stokes shifts, and high fluorescence yields, characteristic of BODIPY-labeled probes [185].

1.7 Dehydroergosterol (DHE)

A naturally-occurring fluorescent sterol analog, dehydroergosterol (DHE), was found in the membranes of eukaryotes such as the yeast *Candida tropicalis* [186], the yeast *Saccharomyces cerevisiae* [187], and the Red Sea sponge *Biemna fortis* [188]. As a result of its natural occurrence and intrinsic fluorescence, its physical properties have been studied [189] and many investigations undertaken to analyze its characteristics in crystals [122, 124, 190], in model membranes (reviewed in [128, 157, 160, 190–192]), in biological membranes (reviewed in [3, 84–86, 97, 135, 193–196]), and its associations with proteins (reviewed in [162, 193, 197, 198]) including the lipoproteins (reviewed in [199, 200]). Fluorescence resonance energy transfer (FRET) between protein-bound DHE donor and cholesterol binding protein aromatic amino acid acceptor has been used to determine the intermolecular distance between these residues within the sterol binding site [160, 190, 197, 201]. In studies with cultured cells, DHE replaced up to 85% of endogenous cholesterol and had no significant effect on viability of L-cell fibroblasts, CHO cells, macrophages, hepatic cells, or MDCK cells [4, 148, 180, 202–205]. DHE codistributed with cholesterol in the plasma membrane and intracellular membranes and did not affect membrane phospholipid composition, membrane sterol/phospholipid ratio, or function of sterol sensitive enzymes in the plasma membrane [148]. In studies to determine the sterol-structure specificity of cholesterol-sensitive membrane receptors (e.g., oxytocin receptor), when membranes were depleted of cholesterol receptor activity was abolished, but when different sterols were added back, as methyl-β-cyclodextrin complexes, to reconstitute activity only cholesterol and DHE were able to restore nearly all function [206–208]. Finally, as lipid rafts/caveolae have become the subject of intense scrutiny over the past decade DHE has increasingly been employed to examine the static and dynamic properties of sterol in these domains within plasma membranes, both *in vitro* and in living cells [4, 13, 128, 205]. Recent developments in microscopic imaging techniques have enhanced the ability to observe DHE in living cells through conventional or video fluorescence microscopy using ultraviolet excitation [162, 180, 202–204] and by multiphoton laser scanning microscopy (MPLSM) [3, 129, 209, 210].

DHE has a conjugated triene system (Figure 1.2B) which gives the sterol probe an excitation maximum at 324 nm and an emission maximum at 371 nm in ethanol (Table 1.1) but the emission maximum shifts to 404 nm in aqueous buffer [128] because of the formation of microcrystals (Table 1.1). Only a small shift is seen in the absorption or excitation spectrum of the DHE in aqueous buffer, potentially due to the polar environment, but a much larger effect is seen in the emission spectrum. An apparent excimer interaction between DHE molecules within the crystalline structure causes a significant enhancement of the longer wavelength electronic levels [128]. The spectrum reveals a fourfold increase in the quantum efficiency [128] over the quantum efficiency (0.04) measured in ethanol [189]. In solvents such as chloroform or acetone, the quantum yield was reduced dramatically [189]. The ultraviolet excitation of DHE has made imaging by conventional fluorescence microscopy or confocal laser scanning microscopy (CLSM) in living cells difficult

due to the potential ultraviolet radiation damage and the need for UV optics, not to mention the high photobleaching rate and low quantum yield [162, 189].

Nevertheless, the fact that DHE is a naturally-occurring fluorescent analog of cholesterol spurred interest such that DHE was eventually imaged successfully in single photon mode at lower excitation intensities using a video imaging approach wherein high ultraviolet (UV) transmissive optics and appropriate filter sets were used in conjunction with a cooled back-thinned charge coupled device (CCD) camera with a high quantum efficiency of detection [180, 202]. Initially, the DHE was delivered to the CHO cells from an ethanol stock solution but difficulties due to aggregation required removal of DHE aggregates by treating the cells with trypsin and extensive washing and centrifugation [180]. In order to facilitate dynamical studies involving DHE intracellular transport, a pulse-chase method utilizing MβCD-DHE complexes was shown to be more effective for quickly loading the plasma membrane with the fluorescent sterol [202–204, 211, 212]. DHE loaded in this manner was shown to colocalize with transferrin in a modified CHO cell line, indicative of DHE distributing into the endocytic recycling compartment (ERC) [211]. Further observations concluded that the DHE transport from the plasma membrane to the ERC was energy independent while transport back to the plasma membrane was vesicular. The results were corroborated using [^{3}H]-cholesterol and ^{125}I-Transferrin isolation techniques [211]. These data suggest that at least some plasma membrane sterol enters the cells by endocytic mechanisms (e.g., clathrin-coated pits) not involving lipid rafts.

In polarized HepG2 human hepatoma cells, DHE delivered to both apical and basolateral membranes was rapidly transferred to the apical membrane through the subapical or apical recycling compartment with very little transfer to the trans-Golgi network [202]. Dehydroergosterol was also incorporated into HDL wherein the apolipoprotein was labeled with the Alexa 488 fluorophore [204]. Using this approach in polarized HegG2 cells, DHE and the Alexa 488-labeled HDL were observed, after 1 min incubation at 37 °C, to accumulate in the bile canaliculus (labeled with rhodamine dextran) within minutes [204]. Interestingly, if the cells underwent depletion of ATP, whereupon uptake of the Alexa 488-HDL and also Alexa 546-Tf (transferrin) was completely blocked, DHE with higher labeling of the basolateral membrane was still observed to accumulate in the bile canaliculus [204], once again indicative of non-vesicular transport. In this study using dehydroergosterol and fluorescence imaging, scavenger receptor class B type I (SR-BI) was observed to mediate the uptake of the HDL-DHE [204]. Other imaging-based techniques, large area fluorescence recovery after photobleaching (FRAP) and fluorescence loss in photobleaching (FLIP) experiments, were performed on DHE in polarized HepG2 cells to study transport in the bile canaliculus and basolateral membrane, revealing a non-vesicular transport pathway [202].

DHE has been incorporated into L-cell fibroblasts where it has been shown to replace nearly 85% of the intracellular cholesterol and maintain cell viability [191]. Incorporation of the probe can be performed using each of the three methods: direct, LUVs, or DHE-MβCD complexes. Direct addition to aqueous buffers creates aggregates of DHE monohydrate crystals which L-cells will phagocytose

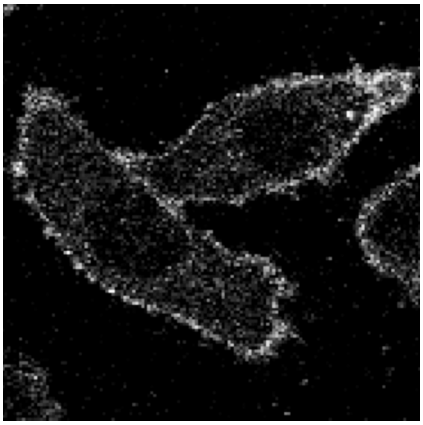

Figure 1.8 Multiphoton laser scanning microscopy of DHE-MβCD in living cells. DHE-MβCD complexes were prepared as described in the Methods. L-cells on chambered cover glass were incubated with the DHE-MβCD complexes (DHE concentration at 20 μg ml^{-1}) in PBS at room temperature for 45 min and imaged. Laser excitation was tuned to 900 nm and the emission was collected using non-descanned detectors and a D400/100 (~350–450 nm) emission filter.

over time. When imaged by MPLSM, the microcrystals show up brightly due to enhanced longer wavelength emission with a much weaker intensity of the plasma membrane [128]. However, cells can be incubated with LUVs containing DHE which can then fuse to the plasma membrane. DHE taken up this way presents as mostly monomeric under typical conditions [128]. Similarly, cells reveal mostly monomeric emission under uptake by DHE-MβCD complexes (Figure 1.8) with fairly rapid uptake rates, of the order of minutes as opposed to hours. Once it has been verified that monomeric dehydroergosterol has occurred within the living cells, emission filters with broader bandwidth can be used to enhance detection over the emission range of DHE to extend the range of experiments that can be performed.

Previously, few techniques have been applied to directly image the distribution of a suitable cholesterol analog and these did not utilize the optical sectioning ability of multiphoton lasers combined with laser scanning microscopy [213–216]. Now, real-time multiphoton laser scanning microscopy (MPLSM) has been applied to DHE in the plasma membrane of living cells to produce new data and results [124, 128, 129, 162, 209, 217]. MPLSM imaging studies have revealed that there is not a uniform distribution of sterol within the plasma membrane of living murine L-cell fibroblasts [3, 128, 129, 209]. There are regions of high and low concentrations of the DHE, with the DHE-rich regions colocalizing with lipid raft markers. Since the diffraction limit of optical laser microscopy resolution is ~200 nm, the exact nature of the microdomains could not be elucidated. For instance, were the high intensity regions, as represented by several pixels, contiguous lateral sterol domains? In order to further characterize these areas in a more global approach, computerized segmentation techniques along with inference statistics were used to examine the plasma membrane distribution. It was revealed that the sterol-rich regions were

distributed non-randomly with evidence of clustering. Estimation of the range of the "macro-level" clustering process was 200–565 nm [209].

1.8
22-(p-Benzoylphenoxy)-23,24-bisnorcholan-5-en-3β-ol (FCBP) Photoactivatable Sterol

This cholesterol analog (Figure 1.2G) with photoactivatable benzophenone group, FCBP, has been synthesized and a radiolabeled version ^{3}H-FCBP prepared [125, 218]. Absorption (Figure 1.9A) and emission spectra (Figure 1.9B) of the FCBP [219] revealed that CLSM was not a realistic possibility due to the UV excitation wavelengths <300 nm and monomeric emission ~330 nm (Table 1.1) with non-detectable emission in aqueous buffer. On examination of the emission spectrum of the FCBP-MβCD complex (Figure 1.9B), a significant amount of the excimeric emission [220] was observed as well as some shift in emission wavelength (compare Table 1.1). With regards to microscopic imaging in living cells FCBP was a good candidate for multiphoton excitation (MPLSM) but the fluorescence of the monomeric emission in the UV was below the transmission of the microscope optics, including the objective. The excimer emission, however, was shifted into the visible. This was demonstrated by MPLSM imaging as the intracellular fluorescence of the excimer appeared brightly within living cells. The L-cells were labeled by two methods: overnight incubation in the dark with LUVs containing FCBP (Figure 1.9C) or 30 min incubation with FCBP-MβCD complexes (Figure 1.9D).

Previous studies replaced ~50% of the free cholesterol with the ^{3}H -FCBP in smooth muscle cells during long incubation times (2 days) without dramatic effect upon the cells [125]. Sterol efflux kinetics using apo A-I were similar for ^{3}H -cholesterol and the ^{3}H -FCBP for times up to 5 h. As a result of the stability of the benzophenone group and its ability for UV activation for crosslinking to amino acid α-carbon atoms, further experiments were performed using the smooth muscle cells. These showed that ~25% of the ^{3}H -FCBP cross-linked to caveolin-1 [125]. The ^{3}H -FCBP was also found in other molecular weight fractions presumably cross-linked to other unidentified proteins in the range 14–150 kDa [125]. In a comparison, using ^{3}H -cholesterol and ^{3}H -FCBP, sterol associated with caveolin-1 decreased in 4–5 h incubation with apolipoprotein A-I (apo A-I) which corresponded to increases in sterol associated with the apo A-I [125].

1.9
BCθ

BCθ, though not a fluorescent sterol itself, has been found to bind cholesterol and so has been found useful in imaging cholesterol distributions in the plasma membrane (Figure 1.10). BCθ was derived by biotinylation of the protease-nicked θ-toxin [126, 127], a cytolysin of *Clostridium perfringens* [126, 127, 221–224]. θ-toxin, or perfringolysin O, has been categorized within a group of thiol-activated hemo-